

# Shining Light on the Microscopic Resonant Mechanism Responsible for Cavity-Mediated Chemical Reactivity

Christian Schäfer<sup>1,2,3,4,\*</sup>, Johannes Flick<sup>5,7,†</sup>, Enrico Ronca<sup>6,‡</sup>, Prineha Narang<sup>7,§</sup> and Angel Rubio<sup>1,2,5,¶</sup>

<sup>1</sup> *Max Planck Institute for the Structure and Dynamics of Matter and Center for Free-Electron Laser Science & Department of Physics, Luruper Chaussee 149, 22761 Hamburg, Germany,*

<sup>2</sup> *The Hamburg Center for Ultrafast Imaging, Luruper Chaussee 149, 22761 Hamburg, Germany*

<sup>3</sup> *Department of Physics, Chalmers University of Technology, 412 96 Göteborg, Sweden*

<sup>4</sup> *Department of Microtechnology and Nanoscience, MC2, Chalmers University of Technology, 412 96 Göteborg, Sweden*

<sup>5</sup> *Center for Computational Quantum Physics, Flatiron Institute, New York, New York 10010, United States,*

<sup>6</sup> *Istituto per i Processi Chimico Fisici del CNR (IPCF-CNR), Via G. Moruzzi, 1, 56124, Pisa, Italy,*

<sup>7</sup> *John A. Paulson School of Engineering and Applied Sciences, Harvard University, Cambridge, Massachusetts 02138, USA*

(Dated: April 27, 2021)

Strong light-matter interaction in cavity environments has emerged as a promising and general approach to control chemical reactions in a non-intrusive manner. The underlying mechanism that distinguishes between steering, accelerating, or decelerating a chemical reaction has, however, remained thus far largely unclear, hampering progress in this frontier area of research. In this work, we leverage a combination of first-principles techniques, foremost quantum-electrodynamical density functional theory, applied to the recent experimental realization by Thomas et al. [1] to unveil the microscopic mechanism behind the experimentally observed reduced reaction-rate under resonant vibrational strong light-matter coupling. We find that the cavity mode functions as a mediator between different vibrational eigenmodes, transferring vibrational excitation and anharmonicity, correlating vibrations, and ultimately strengthening the chemical bond of interest. Importantly, the resonant feature observed in experiment, theoretically elusive so far, naturally arises in our investigations. Our theoretical predictions in polaritonic chemistry shine new light on cavity induced mechanisms, providing a crucial control strategy in state-of-the-art photocatalysis and energy conversion, pointing the way towards generalized quantum optical control of chemical systems.

## I. INTRODUCTION

In recent years, strong light-matter interaction [2–5] has experienced a surge of interest in chemistry and material science as a fundamentally new approach for altering chemical reactivity and physical properties in a non-intrusive way. Seminal experimental and theoretical work has illustrated the possibility to control photo-chemical reactions [6–11] and energy transfer [12–21], strongly couple single molecules [22–27] or extended systems [28–30], and even modify superconductivity [31, 32]. Vibrational strong-coupling is a particularly striking example. For instance, it was observed that coupling to specific vibrational excitations can inhibit [1, 33], steer [34], and even catalyze [35, 36] a chemical process. While experimental work continues to make strides, a theoretical understanding of the mechanism that controls chemical reactions *via* vibrational strong-coupling still remains largely unexplained, a critical gap that our work here closes. Initial attempts to describe vibrational strong-coupling in terms of equilibrium transition-state theory [37–39]

have suggested no dependence on the cavity frequency, in stark contrast with the experimental observations. A second approach suggesting an effective dynamical caging by the cavity [40] partially introduced frequency dependence, but so far has been unable to connect to the experimentally observed frequency dependence.

In this work, we report for the first time a comprehensive picture of the microscopic resonant mechanism responsible for cavity-mediated chemical reactivity and excellent agreement of *ab initio* calculations with experimental observations [1, 33]. Specifically, we observe the inhibition of the deprotection reaction of 1-phenyl-2-trimethylsilylacetylene (PTA) presented in Ref. [1] and schematically illustrated in Fig. 1. Our *ab initio* investigations give rise to the same resonant condition observed in experiment without the presence of a solvent, thus resolving a recent debate questioning previous experimental investigations [41, 42]. While further investigations will be necessary to entirely resolve the effects behind vibrational strong-coupling, we provide critical theoretical evidence to settle an unresolved and active debate in the field [1, 37–39, 41, 42], suggesting that strong-coupling to specific vibrational modes can indeed modify chemical reactivity.

Our approach relies on the recently introduced quantum-electrodynamical density-functional theory (QEDFT) framework [43–49] that enables the full description of electronic, nuclear and photonic degrees

\* Electronic address: christian.schaefer.physics@gmail.com

† Electronic address: jflick@flatironinstitute.org

‡ Electronic address: enrico.ronca@pi.ipcf.cnr.it

§ Electronic address: prineha@seas.harvard.edu

¶ Electronic address: angel.rubio@mpsd.mpg.de

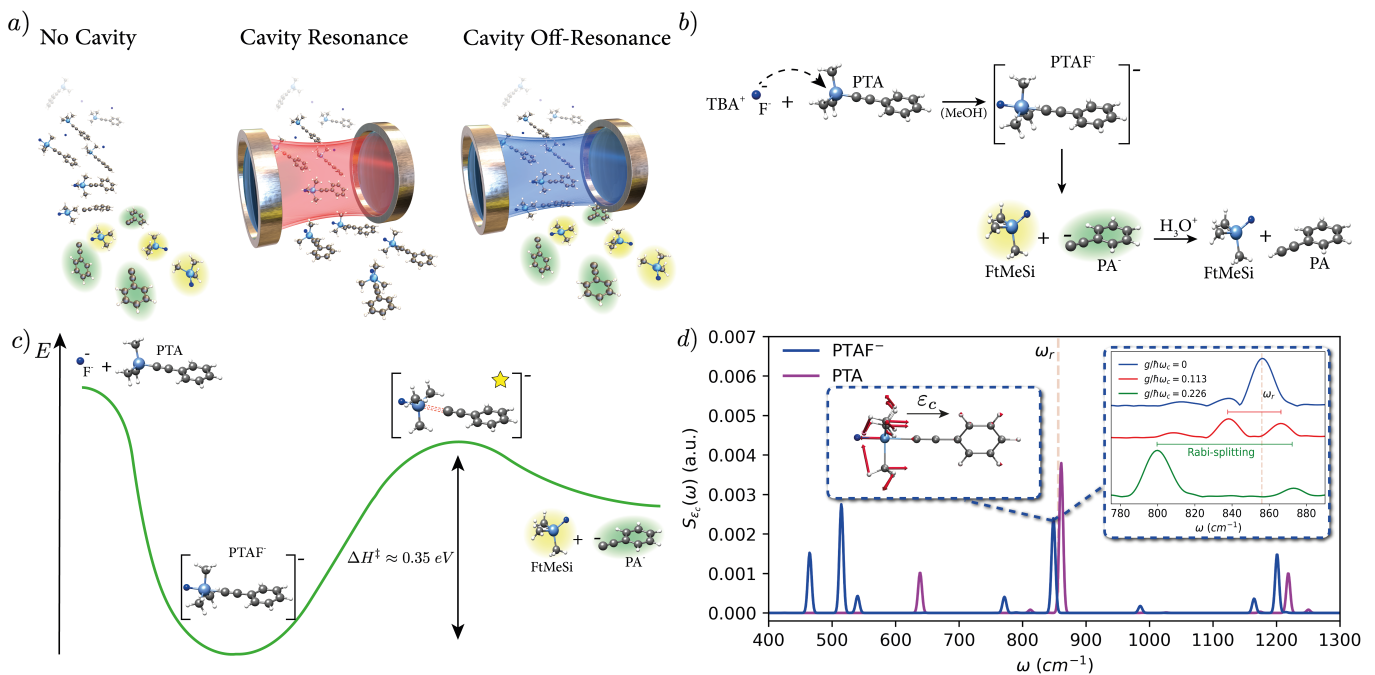


**FIG. 1.** (a) Resonant vibrational strong-coupling can inhibit chemical reactions. (b) Illustration of the reaction mechanism for the deprotection of 1-phenyl-2-trimethylsilylacetylene (PTA), with tetra-*n*-butylammonium fluoride (TBAF) and (c) energetic of the reaction in (b) in free-space. The successful reaction involves breaking the Si-C bond and thus overcoming a transition-state barrier of 0.35eV. (d) Vibrational absorption spectrum along the cavity polarization direction  $S_{\epsilon_c}(\omega) = 2\omega \sum_{j=1}^{N_{vib}} |\epsilon_c \cdot \mathbf{R}(\omega_j)|^2 \delta(\omega - \omega_j)$  illustrating the strong-coupling of the vibrational eigenmode at 856 cm<sup>-1</sup> with the cavity polarized along  $\epsilon_c$  for PTAF<sup>-</sup> (blue) and the isolated PTA complex (magenta). The insets show the coupled vibrational mode and the light-matter hybridization under vibrational strong-coupling. Our time-dependent calculations describe the correlated (non-adiabatic) movement of electrons, nuclei and cavity field during the reaction.

of freedom from first principles. QEDFT recovers the resonant dynamic nature of the chemical inhibition under vibrational strong-coupling, illustrating the strength embodied by first-principle approaches in this context. We find that the cavity introduces an additional coupling between the molecular vibrational modes, leading to new anharmonic vibrations. By virtue of the new basis of eigenmodes (mixed cavity-vibrational modes), the original vibrational modes of the system become increasingly correlated enabling new paths for the energy to be redistributed. Energy deposited in a single bond during the reaction quickly spreads to the set of correlated modes such that the probability to break a specific bond is diminished. For increasing light-matter interaction a second mechanism attains increasing relevance. The cavity enacts an repellent force on the F<sup>-</sup> attacking the PTA complex due to the induced molecular currents. Consequently, the speed of the reaction reduces and the probability to follow the common reaction pathway is diminished.

## II. REACTION MECHANISM AND RESONANT VIBRATIONAL STRONG-COUPLING FROM FIRST-PRINCIPLES

Under typical reaction conditions, that is, no vibrational strong-coupling, the deprotection reaction of 1-phenyl-2-trimethylsilylacetylene (PTA) with tetra-*n*-butylammonium fluoride (TBAF) to give phenylacetylene (PA) and fluorotrimethylsilane (FtMeSi) is expected to evolve (see fig. 1 b) as follows [1, 50, 51]. In solution (usually methanol) the F<sup>-</sup> ions released by TBAF form an intermediate pentavalent complex (PTAF<sup>-</sup>) that reduces considerably the barrier for the dissociation of the Si-C bond, inducing the exit of the phenylacetylide anion (PA<sup>-</sup>). In solution a fast protonation of the PA<sup>-</sup> brings to the formation of the final phenylacetylide (PA) product. Here, we will describe the explicit evolution of the reaction for a single molecule represented by an ensemble of thermally distributed independent trajectories that follow the equations of motion provided by (quantum-electrodynamical) density-functional theory. Our numerical investigations start from the PTA+F<sup>-</sup> initial state over the intermediate pentavalent PTAF<sup>-</sup> complex up to the breaking of the Si-C bond (see fig. 1 c), thus explicitly including the rate limiting step (PTA+F<sup>-</sup> → FtMeSi + PA<sup>-</sup>).

In order to simulate vibrational strong-coupling inside the cavity and its effect on the reaction, we couple a single cavity mode with variable frequency  $\omega_c$ , effective cavity volume  $V_c$ , and fixed polarization  $\epsilon_c$  to the molecular dipole moment  $\hat{\mathbf{R}}$  according to  $\hat{H} = \hat{H}_{\text{Matter}} + \hbar\omega_c(\hat{a}^\dagger\hat{a} + \frac{1}{2}) + \sqrt{\frac{\hbar\omega_c}{2\epsilon_0 V_c}}(\epsilon_c \cdot \hat{\mathbf{R}})(\hat{a}^\dagger + \hat{a}) + \frac{1}{2\epsilon_0 V_c}(\epsilon_c \cdot \hat{\mathbf{R}})^2$  [48, 52, 53]. The dimensionless ratio  $g/\hbar\omega_c$  with coupling  $g = ea_0\sqrt{\hbar\omega_c/2\epsilon_0 V_c}$  provides an indication for relative light-matter coupling strengths. We select interaction strengths that result in hybridization (or Rabi) splittings of around 10% and therefore on the order of the experimentally observed spectra (see fig. 1 d). The specific value chosen here does not influence the qualitative observation and we will discuss in the following how such local effective couplings could emerge. Retaining the quadratic operator  $\frac{1}{2\epsilon_0 V_c}(\epsilon_c \cdot \hat{\mathbf{R}})^2$  is however critical to ensure a physically sound result [53]. The correlated evolution of electronic, nuclear, and photonic system is described by quantum-electrodynamical density-functional theory employing Maxwell's equation of motion [24, 48, 54] (details in Materials and Methods V).

A prerequisite for reactive control is the strong-coupling condition, that is, a hybridization energy between vibration and photon larger than the combined decoherence of the system. Intuitively, the cavity excitation would be overlaid with a vibrational excitation and the hybridization correspondingly visible. Obtaining vibro-polaritonic spectra and confirming the strong-coupling condition is thus a first essential step in any *ab initio* QED chemistry investigation. Fig. 1 d illustrates the vibrational absorption spectrum along the cavity polarization axis for isolated PTA and pentavalent  $\text{PTAF}^-$  complex. Clear resonances around  $\omega_r = 856 \text{ cm}^{-1}$  can be observed, suggesting that the vibrational strong-coupling conditions are met around the local minimum ( $\text{PTAF}^-$ ) as well as for all molecules previous to any reaction (PTA).

During the reaction, however, the molecular geometry and its vibrational spectrum change considerably (more details in Materials and Methods V) such that simulations involving a single molecule are unlikely to exhibit a sharp resonant condition for an effect of the cavity on the reaction. In addition, the Si-C bond of special interest contributes to a set of vibrational eigenmodes which are distributed over a wide frequency-range. In combination, retaining exact resonance between a specific cavity mode and a specific vibrational mode during the reaction is virtually impossible but also not necessary as we will confirm in the following the experimentally observed effect including its resonant condition. Our investigations illustrate that reduced model descriptions, while powerful and intuitive in many situations, can be misleading at times and that first principles calculations are essential in the future understanding and development of polaritonic chemistry.

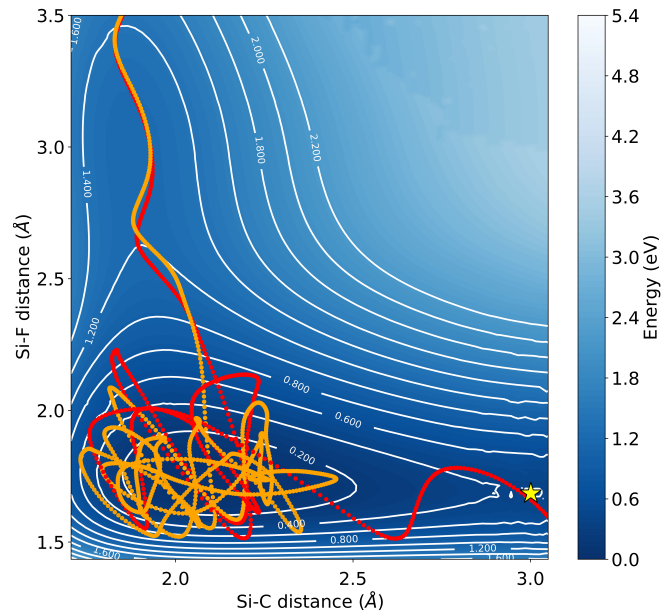


**FIG. 2.** Exemplary trajectory outside  $g/\hbar\omega_c = 0$  (red) and inside the cavity  $g/\hbar\omega_c = 0.283$ ,  $\omega_c = 856 \text{ cm}^{-1}$  (orange) undergoing the reaction illustrated in fig. 1 (b, c). The transition-state is indicated with a yellow star. Encoded in the transparency is the relative angle between Si-C and cavity polarization axis (inset fig. 1 d). The molecular axis remains largely oriented along the cavity polarization during the reaction.

### III. CAVITY INDUCED INHIBITION OF A GROUND-STATE CHEMICAL REACTION

In order to identify the physical mechanism behind the cavity induced inhibition of the Si-C bond-breaking, we perform real-time quantum-electrodynamical density-functional theory calculations for a set of 30 trajectories which are launched with initial conditions sampled from a thermal distribution at 300 Kelvin. Fig. 2 illustrates one such exemplary trajectory in free-space (red) and when strongly coupled to the resonant cavity-mode (orange). The potential energy surface is shown here for illustrative purposes only and has not been employed in the propagation. For the given set-up, the way  $\text{F}^-$  attaches and how the pentavalent  $\text{PTAF}^-$  complex is formed is barely disturbed. Once the molecule enters the pentavalent complex, a clear change in the dynamics of the Si-C bond is observed. The resonant cavity effectively traps the system around the local minimum, extending the reaction-time beyond the simulation time of 1 ps by protecting the Si-C bond from dissociating.

To further elucidate the bond-strengthening feature of the cavity, we project the dynamical nuclear-coordinates during the time-dependent evolution on the vibrational eigenmodes of the bare  $\text{PTAF}^-$  system (without cavity). Illustrated in fig. 3 is the absolute difference of mode occupation between strong resonant coupling  $\omega_c = 856 \text{ cm}^{-1}$  and far off-resonant coupling  $\omega_c = 425 \text{ cm}^{-1}$ . Particularly relevant is the time-domain in which the F

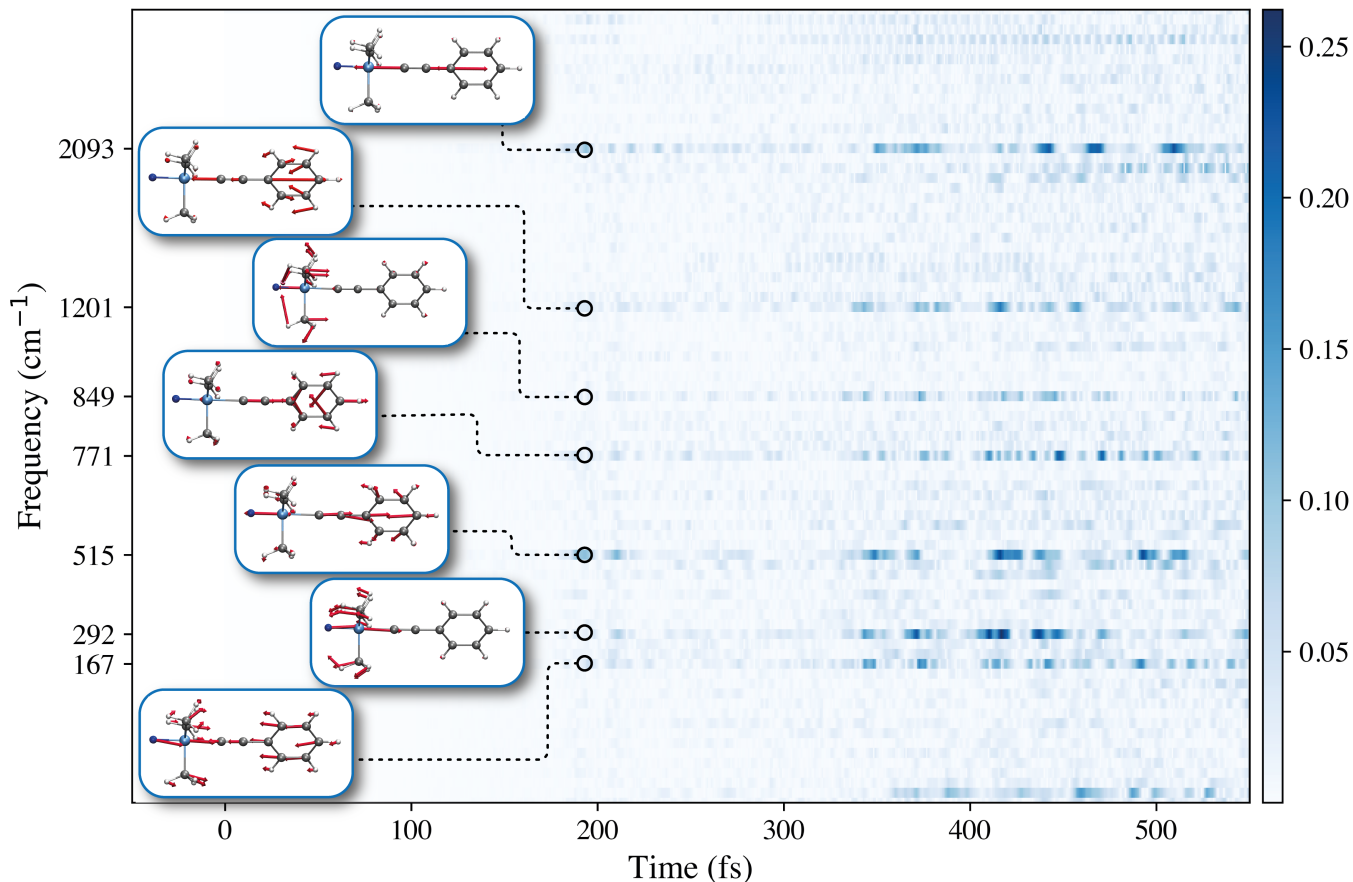


**FIG. 3.** Time-resolved influence on the mode occupations by resonant vibrational strong-coupling. Illustrated is the trajectory averaged absolute difference in normalized mode-occupation between on resonant condition  $\omega_c = \omega_r = 856 \text{ cm}^{-1}$  and far off-resonance  $\omega_c = 425 \text{ cm}^{-1}$  for all trajectories that undergo the reaction at  $\omega_c = 425 \text{ cm}^{-1}$ .

anion attaches to PTA at 200 fs and the Si-C bond-breaking in free-space at 500 fs. The latter is foreshadowed by increasing occupations in modes involving vibrations of the F-Si-C-C chain. Without surprise, many (anharmonic) vibrational modes contribute to the reaction, rendering it challenging to describe the reaction in terms of a reduced subset of coordinates. While the cavity has an overall minor effect on the vibrational occupations in the aforementioned time-window, it leads to considerable redistribution of occupation in modes along this F-Si-C-C chain. Consequently, the cavity can prevent the bond-breaking of Si-C by distributing energy into other vibrations along the F-Si-C-C chain, effectively correlating the vibrations along the chain. The dominant effect of vibrational strong-coupling on a ground-state chemical reaction would be therefore that it provides means to redistribute the energy from a specific bond into other degrees of freedom. These observations suggest a clear dependence on the symmetry of the molecule and associated reaction pathways, in conceptually close agreement with recent experimental investigations [55].

We acknowledge that such correlations *via* the cavity-mode would necessarily depend on the chemical complex, reaction mechanism and ambient conditions. Our results

and experimental observations [1, 33, 34] suggest, however, that tuning the cavity in resonance to a molecular vibrational excitation with relevant contribution to reactive bonds prefers to inhibit typically dominant reaction pathways. In our investigations, the inhibition of the reaction for a given temperature can be overcome by increasing the molecular temperature to the point that the energetic redistribution mediated by the cavity becomes negligible. Each pathway affected by the cavity would then become increasingly sensitive to thermal changes. This provides room for other usually suppressed pathways, leads to an overall tilt in the reactive landscape, and alters the thermodynamic characteristics of the reaction. The way that catalytic effects *via* vibrational strong-coupling to solvents [35, 36] follow the same rationale and pathway remains an open question.

The experimental conditions [1, 33–36] suggest an involvement of a macroscopic number of molecules  $N$  that collectively couple to the cavity excitation, effectively representing a set of synchronized oscillators leading to a  $\sqrt{N}$  enhancement of the effect. Such a collective interaction does not necessarily imply that a single molecule is strongly affected by the light-matter interaction as shown here. Recent theoretical work suggests however that col-



lective strong-coupling can lead to local strong-coupling as the individual molecule undergoing the reaction experiences a collectively enhanced dipole moment [56, 57]. In addition to the here observed intra-molecular energy redistribution, inter-molecular interactions mediated by the cavity might further inhibit accumulation of energy in specific bonds, thus preventing specific reactions. Experimental ambient conditions influence the coherence of those processes and will likely determine the relevance of intra- and inter-molecular vibrational energy redistribution. Further, intra- and inter-molecular processes should obey a different dependence on the symmetry of the molecule. The combination of both ‘handles’ could provide a possible path to elucidate their individual relevance in vibrational strong-coupling.

### A. Observation of a Resonant Effect

While experiments so far have indicated a clear dependence on the resonant conditions between vibration of interest and cavity, theory has not been able to agree with this as a critical prerequisite. Hidden in the overall debate (and disagreement with previous predictions) are two aspects that are combined in a single experimental observation. The first is the strong-coupling condition itself. When decoherences dominate the energy exchange between vibrations and photons, their hybridization vanishes and no relevant effect of the cavity environment on the chemical reaction can be observed [1]. This implies that the possibility of modifying the chemical reaction should closely follow the strong-coupling condition. Second, the vibrations that dominantly contribute to the bond-breaking have to be involved in this strong-coupling condition.

In our *ab initio* theoretical investigation, the strong-coupling condition is always fulfilled, and thus we dominantly investigate the second resonant condition. By varying the length of the idealized Fabry-Pèrot cavity, we tune the frequency of the cavity mode while keeping the ratio between coupling and frequency  $g/\hbar\omega_c$  constant. Fig. 4 illustrates our extensive *ab initio* calculations addressing the resonant effect in a compact trajectory averaged form. We show the trajectory averaged Si-C distance over time (a) in addition to the time-averaged Si-C distance (b) and its variance (c) averaged over all trajectories. The majority of the trajectories exhibit a clear resonant feature around the experimentally observed resonant frequency at  $860\text{ cm}^{-1}$ . While the vibrational spectra for the relaxed structures of PTA and PTA $F^-$  are only overlaying with the cavity frequency at  $856\text{ cm}^{-1}$ , the spectra change considerably for non-relaxed configurations, e.g. the initial state PTA+F (see Materials and Methods V). As a consequence, cavity frequencies close to the aforementioned  $856\text{ cm}^{-1}$  can momentarily couple to dynamically changing normal-modes during the reaction and might explain the broadened resonant behaviour in fig. 4. We, therefore, find that the suggested

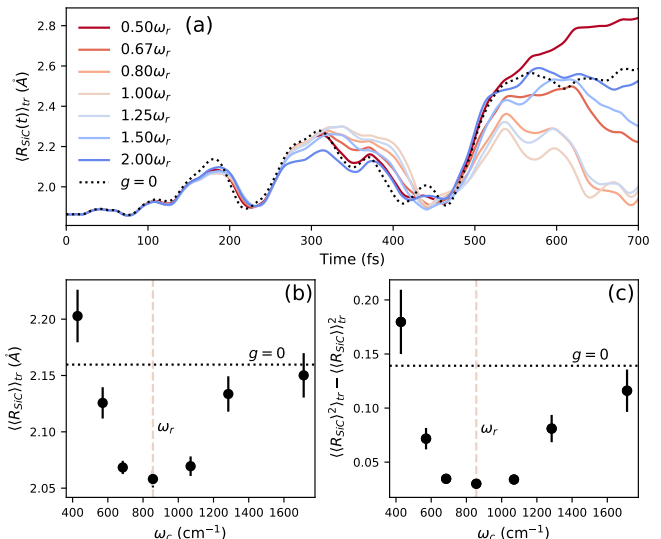


**FIG. 4.** Time-resolved trajectory averaged Si-C distance (a, top) and time-averaged Si-C distance (b) and variance (c) for varying cavity frequency  $\omega_c$  relative to the resonant frequency  $\omega_c = \omega_r = 856\text{ cm}^{-1}$ . The ratio  $g/\hbar\omega_c = 0.283$  is kept constant. Error-bars show the standard error of the trajectory average. The Si-C bond breaks at around 500 fs in free-space (black dotted) while under resonant conditions a clear inhibition manifests. We observe that close to resonance, a small set of trajectories will undergo the reaction at longer times (more details in App. C). At  $\omega_c = 0.5\omega_r$  the statistical ensemble would need to be extended for further conclusions.

effective strengthening of the Si-C bond, emerging from funneling vibrational energy *via* the cavity away from the Si-C bond into other degrees of freedom, agrees well with the experimental observations. A second mechanism for the inhibition of the reaction appears at higher frequencies. Larger frequencies imply smaller mode-volumes and higher fundamental coupling as  $g/\hbar\omega$  is kept constant. This can lead to a cavity-induced repellent force on the approaching  $F^-$  as will be discussed in Sec. III B.

To observe this resonant effect at all, the kinetic nature of the reaction seems to play a much more significant role than commonly perceived for ground-state reactivity where transition-state theory is a common practice. First investigations following equilibrium transition-state theory suggested that the cavity frequency has no significant influence on the reaction rate [37–39]. Attempts to explain the resonant character in terms of a dynamical caging effect [40] suggested a resonant frequency of  $74\text{ cm}^{-1}$  (for further details see App. B). Our quantum-electrodynamical density-functional theory on the other hand seamlessly provides the experimentally observed resonant condition, suggesting that first-principles techniques provide indeed a valuable and needed addition to the theoretical tool-set. Further investigations will focus on the thermodynamic influence of the here reported observations.

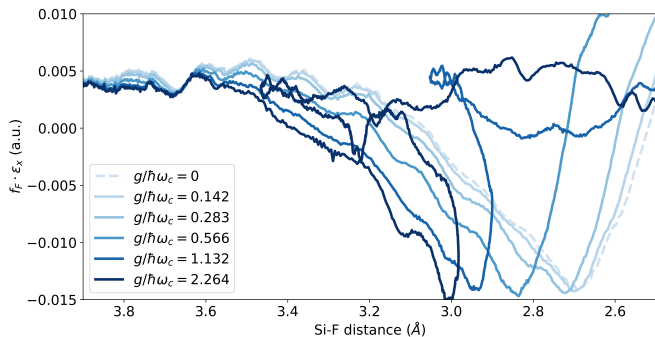


**FIG. 5.** Force acting on the F atom along the cavity polarization axis for the **2** corresponding trajectory. With increasing light-matter coupling a cavity induced repellent force emerges preventing the F anion to attack the PTA complex. The Maxwell coupling utilized here becomes less reliable for larger coupling strength.

### B. Preventing the Attachment of $F^-$

When we increase the light-matter coupling strength, two distinct effects can be observed. First, the aforementioned inhibition intensifies, that is, more trajectories will be stronger affected, second the approach of the  $F^-$  anion is delayed. Fig. 5 presents the forces acting on F projected on the cavity polarization axis for increasing light-matter coupling. During the dynamical approach of the  $F^-$  to the PTA complex, the methyl groups of the PTA complex need to rearrange to provide space for  $F^-$ . This leads to a short repellent force acting during the rearrangement time. The approaching  $F^-$  induces noticeable changes in the molecular dipole moment, resulting in an effective nuclear current coupling to the photonic system.

With increasing coupling strength, the latter results in an increasing repulsion which partially prevents  $F^-$  from attaching to PTA. The dynamic change of the molecular dipole with approaching  $F^-$  results therefore in an additional reaction-barrier. Considering that the reaction probability is slim in the first place, the success of  $F^-$  attacking and subsequently the rate of reactions is sensitive to any alternation of the  $F^-$  trajectory. This observation provides another possible explanation for the experimentally obtained large entropic change in the reaction character [1, 33] but would not feature the same dependence on the resonant condition as observed in Sec. III A.

## IV. CONCLUSIONS AND OUTLOOK

Any additional string to guide a reaction on demand might provide an invaluable addition to the chemical toolbox. By leveraging the QEDFT framework, we are able to provide theoretical insight from first-principles into the inhibition of ground-state reactions under vibrational strong-coupling. Our results are in excellent agreement with previous experimental observations [1, 33] and, to the best of our knowledge, for the first time present

the ‘in experiment’ observed resonant condition.

The cavity provides an additional eigenmode to the vibronic system, effectively correlating vibrations. During the reaction, energy is accumulated in specific bonds which in free-space lead to their dissociation. Under strong vibrational coupling, the cavity-correlated vibrations redistribute energy, effectively strengthening the here relevant Si-C bond and ultimately inhibiting the reaction. Our observations are in line with the experimentally observed relevance of symmetry [55] and recover the resonant condition [1, 33] remarkably well.

In agreement with previous studies, we conclude that kinetic features play a much more pronounced role under strong light-matter coupling than commonly assumed for ground-state chemical reactivity. Handles such as symmetry and coherence could elucidate to which extend inter- and intra-molecular energy-redistribution contribute to vibrational strong-coupling. How such kinetically driven effects can persist into the realm of realistic ambient conditions for large ensembles of reacting molecules thus remains a key question necessitating further theoretical and experimental investigations.

## ACKNOWLEDGMENTS

We thank Anoop Thomas, Thomas Ebbesen, Michael Ruggenthaler, and Göran Johansson for insightful discussions. This work was supported by the European Research Council (ERC-2015-AdG694097), the Cluster of Excellence ‘Advanced Imaging of Matter’ (AIM), Grupos Consolidados (IT1249-19), partially by the Federal Ministry of Education and Research Grant RouTe-13N14839, the SFB925 ‘Light induced dynamics and control of correlated quantum systems’, the Swedish Research Council (VR) through Grant No. 2016-06059, the Department of Energy, Photonics at Thermodynamic Limits Energy Frontier Research Center, under Grant No. DE-SC0019140. The Flatiron Institute is a division of the Simons Foundation. P.N. gratefully acknowledges a Moore Inventor Fellowship through Grant GBMF8048 from the Gordon and Betty Moore Foundation and support from the CIFAR BSE Program’s ‘Catalyst’ grant.

## AUTHOR CONTRIBUTIONS

C.S., J.F., and E.R. contributed equally. A.R. and C.S. conceived the project. C.S., J.F., and E.R. obtained and evaluated the data. C.S. prepared a first draft, C.S. and E.R. prepared the figures. All authors discussed the results and edited the manuscript.

## V. MATERIALS AND METHODS

The potential energy surface is obtained using the ORCA code [58] with the 6-31G\* basis set, employ-

ing DFT and the PBE functional. The time-dependent calculations were performed using the highly optimized TDDFT code OCTOPUS [48, 49]. Building the pentavalent complex is entropically unfavored and unlikely such that just a very limited set of trajectories would result in a successful attachment of the F anion. To reduce the amount of non-reactive trajectories we used time-reversal symmetry to estimate the collision speed and angle leading to the reaction. We obtained ideal angles between Si-C and Si-F bond of around 180 degrees. An alternative angle for  $F^-$  to attack Si is at 60 degrees but the latter demands higher temperatures on the order of 900K. Using the linear configuration, we obtained first initial geometries from Orca with a subsequent further optimization in Octopus using a constrained force minimization for a fixed Si-F distance of 4 Å. Starting from those initial geometries, we sample initial velocities according to a Boltzmann distribution at 300 K, i.e., a Gaussian normal distribution with nuclei specific variance  $\sigma_{v_i} = \sqrt{k_b T / M_i}$ . Furthermore, we point the F momentum towards the Si and remove the center of mass movement. We propagate 10 such trajectories and obtain a single reactive trajectory at 300K shown in fig. 2. Then, in order to limit the necessary number of trajectories while still obtaining a reasonable number of reactive trajectories, we sample around the first reactive trajectory a set of 20 additional trajectories with a relative temperature of 20K, removing again the center-of-mass momentum. If not further specified the illustrated observables represent the average of those 30 trajectories. Inside the cavity, the initial photon-mode displacement is provided by the zero-electric field condition  $q(t_0) = -\frac{\lambda}{\omega} \cdot \mathbf{R} \leftrightarrow \mathbf{E}(t_0) = 0$  with  $\dot{q}(t_0) = 0$  and  $\mathbf{R} = \sum_i^{N_n} Z_i \mathbf{R}_i - \sum_i^{N_e} \mathbf{r}_i$  [48, 53, 54]. This initial configuration is then propagated in OCTOPUS [49] using the ETRS (electronic subspace) + velocity verlet (nuclear subspace) time-stepping routine with electronic  $\Delta t_e = 0.0012/eV$  and nuclear  $\Delta t_n = 10\Delta t_e$ . For the electronic subspace, we use the revPBE [59, 60] electronic exchange and correlation potential and the standard SG15 Pseudo-potential set. The nuclear coordinates are moving according to the classical Ehrenfest equations of motion, i.e., electronic and nuclear system are self-consistently enacting forces on each other. The photonic coordinates are coupled via the classical (mean-field) Maxwell light-matter coupling using the QEDFT framework [43–48]. We use a numerical box of  $V = (24 a_0)^3$  and a grid spacing of  $0.24 a_0$  with the bohr radius  $a_0$ . The parameters of the grid are chosen such that numerically caused changes in the energy are minor compared to thermal energies. We monitor the time-evolution of the complex and define the Si-C bond as broken when the Si-C distance increases beyond the transition-state.

Fig. 6 illustrates the vibrational spectrum including the  $PTA+F^-$  initial state and an intermediate strongly stretched state. During the evolution of the reaction, the vibrational modes are constantly changing which allows many more frequencies to dynamically couple to the cavity than the equilibrium PTA or  $PTAF^-$  structures would

suggest. The dynamic shift of the vibrational mode during the reaction clarifies therefore why the resonance is comparably broad.

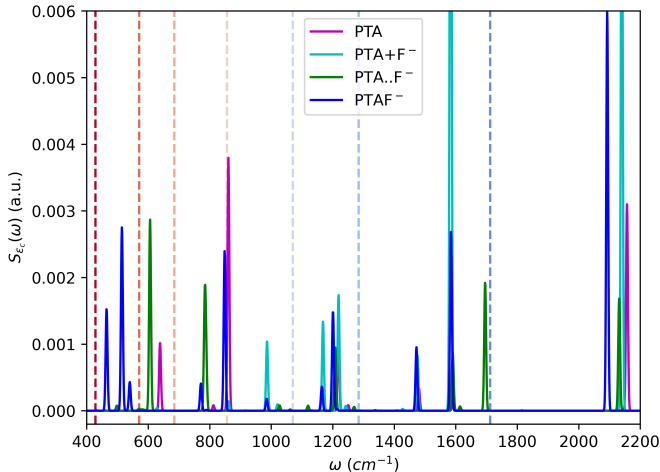


**FIG. 6.** Vibrational absorption spectrum along the cavity polarization direction  $S_e(\omega) = 2\omega \sum_{j=1}^{N_{vib}} |\boldsymbol{\varepsilon}_c \cdot \mathbf{R}(\omega_j)|^2 \delta(\omega - \omega_j)$  for the bare PTA complex (magenta), our initial state  $PTA+F^-$  (cyan), an intermediate state with strongly stretched Si-F bond of 2.889 Å (green), and the pentavalent  $PTAF^-$  complex (blue). Dashed vertical lines indicate the selected cavity frequencies. Vibrational resonances are artificially broadened.

## Appendix A: Discussion of the Energetics and Solvent Effects

In order to eliminate the possibility that the solvent is an integral component of the mechanism that is put forward here, we used ORCA with a continuous PCM model description for the solvent methanol. We obtain the energetic values for reactant  $[PTA+F] = -816.131244 H$ , pentavalent complex  $[PTAF]^- = -816.1943141865 H$ , transition-state  $[PA \dots Me_3SiF] = -816.18146281 H$  and product  $[PA^- + Me_3SiF] = -816.1846728 H$ . We obtain an enthalpy between pentavalent complex and transition-state of  $\Delta H^\ddagger \approx 0.35 eV \approx 34 kJ/mol$  in good agreement with experimental results (30 and 39 kJ/mol) [1, 33]. Ignoring entropic features as well as bond termination with hydrogen, the resulting product is higher in energy than the intermediate step. The experimental investigations suggest that the entropic barrier (54 kJ/mol) is non-negligible. In our simulations, this is expressed in the very narrow window of initial configurations that result in F attaching to PTA and subsequent bond breaking. Thus, the likelihood of the reaction taking place is largely determined by the unlikeliness of a specific initial configuration in addition to the energetic barrier that describes the bond breaking.

In order to estimate if our observations depend critically on the exchange-correlation potential, we calculated the Si-C C=C potential energy surface for the 60% con-

figuration in ORCA using two different basis sets and two different functionals (see fig. 7). While quantitative changes can be observed, they agree qualitatively such that our observations are likely to be robust against changing basis-set or DFT-functional.

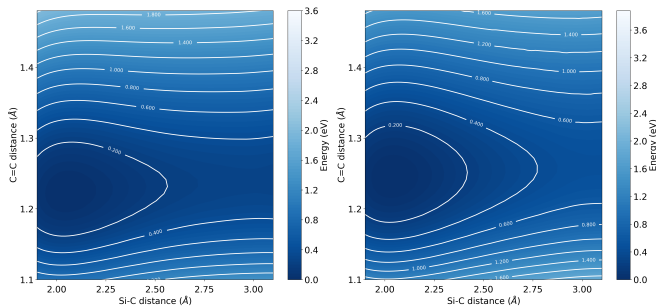


**FIG. 7.** Si-C C=C potential energy surface calculated with ORCA (F out of Si-C axis). Left, using the B3LYP functional and the def2-TZVP basis, right, using the PBE functional and the 6-31G\* basis.

## Appendix B: Curvature at the Transition-state and Resonant Frequencies

Li et al. [40] suggested recently that the resonant effect of the slow down of a reaction under vibrational strong coupling originates from an effective solvent-caging effect around the transition-state. Thereby, the suggested resonant frequency emerges from the curvature of the PES at the transition-state  $M\omega_b^2 = -\partial_R^2 E|_{TS}$ . This would lead to a resonant frequency at  $\omega = 74 \text{ cm}^{-1}$  [40]. Clearly, we observe the same resonant effect as in experiment, i.e., around the same energetic position at  $856 \text{ cm}^{-1}$ . That our dynamical calculations accurately recover the experimentally observed resonance, but correspond to binding frequencies that are orders of magnitude smaller than the experimentally observed resonant condition, suggests that it is not possible to characterize the resonant condition for this reaction by the binding frequency. Both theoretical investigations suggest however plausible explanations for the reduced rate under vibrational strong coupling. It remains then of interest if each mechanism has a dominant regime of validity determined by the character of the reaction, or if a continuous transition in terms of thermodynamic parameters decide the predominant

mechanism.

Table I presents the binding frequency (lowest imaginary vibrational frequency at the transition-state) calculated with ORCA for different solvents, Gaussian basis-sets, and relative orientations of the F anion with respect to the Si-C bond-axis. In addition, we provide relevant resonances, presenting the excellent agreement between QEDFT and experiment.

Theory level	Solvent	F position	$\omega_b$ [ $\text{cm}^{-1}$ ]	Resonance [ $\text{cm}^{-1}$ ]
PBE 6-31G*	Vacuum	in-axis	90	
PBE 6-31G*	Methanol	in-axis	94	
PBE 6-311G*	Methanol	in-axis	88	
B3LYP 6-31G*	Methanol	in-axis	93	
PBE 6-31G*	Acetonitrile	in-axis	94	
PBE 6-31G*	Vacuum	off-axis	85	
PBE 6-311G*	Methanol	off-axis	81	
Li et al. [40]	Methanol	in-axis	74	
QEDFT	Vacuum	in-axis	856	
Experiment	Methanol	-	860	

**TABLE I.** Lowest (imaginary) vibrational frequency at the transition-state for the two different configurations calculated with different solvents and theoretical descriptions. The resonant condition is correctly captured by our QEDFT calculations but not the binding frequency.

## Appendix C: Delay of Reaction without Prevention

The majority of the trajectories undergoing the reaction far off-resonant or in free-space no longer show a reactive behaviour close to resonant conditions. For all of those cases, the trajectory is trapped close to the local minimum at the pentavalent PTAF complex, potentially stretching the Si-C bond but relaxing back to the local minimum. Only a single trajectory undergoes at resonance the reaction but at significantly longer times as fig. 8 illustrates. As the statistical ensemble becomes increasingly insufficient the longer the time-propagation, we decide to limit the presentation of the resonant effect to the first 700 fs. In addition to the exception shown here, close to resonance a smaller set of trajectories undergoes the reaction. Common to all of them is that they demand a longer time to finally break the Si-C bond.

[1] A. Thomas, J. George, A. Shalabney, M. Dryzhakov, S. J. Varma, J. Moran, T. Chervy, X. Zhong, E. Devaux, C. Genet, J. A. Hutchison, and T. W. Ebbesen, Ground-state chemical reactivity under vibrational coupling to the vacuum electromagnetic field, *Angewandte Chemie International Edition* **55**, 11462 (2016).

[2] V. Agranovich, H. Benisty, and C. Weisbuch, Organic and inorganic quantum wells in a microcavity: Frenkel-wannier-mott excitons hybridization and energy transformation, *Solid state communications* **102**, 631 (1997).

[3] V. M. Agranovich, M. Litinskaia, and D. G. Lidzey, Cavity polaritons in microcavities containing disor-



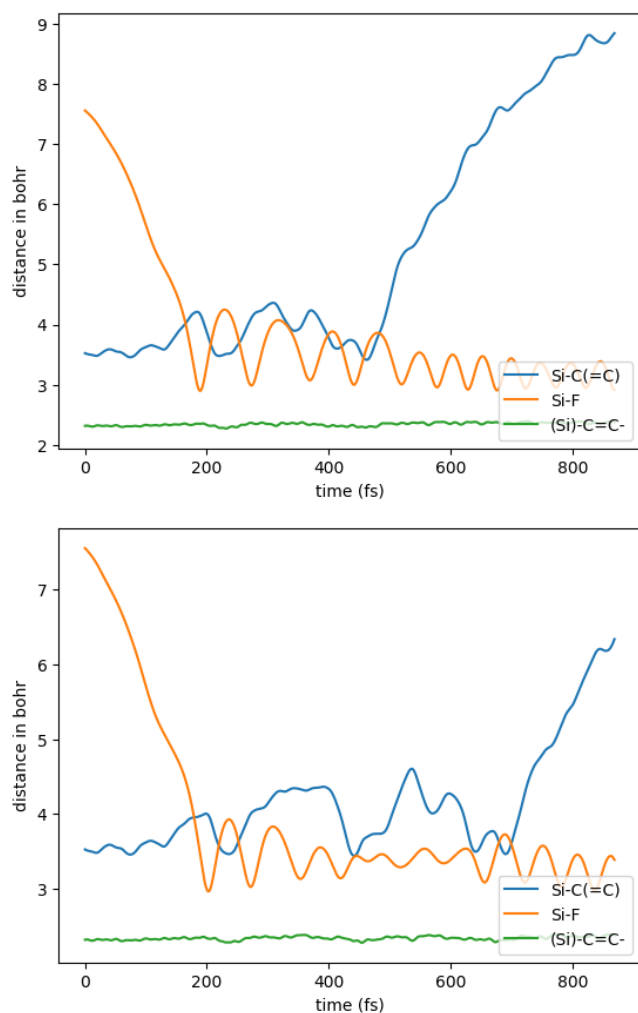


**FIG. 8.** Time-dependent bond distances in free-space (top) and under resonant condition (bottom) for the single outlier trajectory showing the reaction at resonance. The Si-C bond (blue) crosses the transition-state at around 500 fs in free-space and at 800 fs under resonant vibrational strong coupling.

- dered organic semiconductors, *Physical Review B* **67**, 10.1103/physrevb.67.085311 (2003).
- [4] S. Haroche and J.-M. Raimond, *Exploring the quantum: atoms, cavities, and photons* (Oxford university press, 2006).
- [5] E. Power and T. Thirunamachandran, Quantum electrodynamics in a cavity, *Physical Review A* **25**, 2473 (1982).
- [6] J. A. Hutchison, T. Schwartz, C. Genet, E. Devaux, and T. W. Ebbesen, Modifying chemical landscapes by coupling to vacuum fields, *Angewandte Chemie International Edition* **51**, 1592 (2012).
- [7] B. Munkhbat, M. Wersäll, D. G. Baranov, T. J. Antosiewicz, and T. Shegai, Suppression of photo-oxidation of organic chromophores by strong coupling to plasmonic nanoantennas, *Science Advances* **4**, eaas9552 (2018).
- [8] G. Groenhof, C. Climent, J. Feist, D. Morozov, and J. J. Toppari, Tracking polariton relaxation with multiscale molecular dynamics simulations, *The journal of physical chemistry letters* **10**, 5476 (2019).
- [9] J. Galego, F. J. Garcia-Vidal, and J. Feist, Suppressing photochemical reactions with quantized light fields, *Nature Communications* **7**, 13841 (2016).
- [10] M. Kowalewski, K. Bennett, and S. Mukamel, Cavity femtochemistry: Manipulating nonadiabatic dynamics at avoided crossings, *The journal of physical chemistry letters* **7**, 2050 (2016).
- [11] J. Fregoni, G. Granucci, M. Persico, and S. Corni, Strong coupling with light enhances the photoisomerization quantum yield of azobenzene, *Chem* **6**, 250 (2020).
- [12] D. M. Coles, N. Somaschi, P. Michetti, C. Clark, P. G. Lagoudakis, P. G. Savvidis, and D. G. Lidzey, Polariton-mediated energy transfer between organic dyes in a strongly coupled optical microcavity, *Nature Materials* **13**, 712 (2014).
- [13] E. Orgiu, J. A. Hutchison, E. Devaux, J. F. Dayen, B. Doudin, F. Stellacci, C. Genet, J. Schachenmayer, C. Genes, G. Pupillo, P. Samorì, and T. W. Ebbesen, Conductivity in organic semiconductors hybridized with the vacuum field, *Nat. Mater.* **14**, 1123 (2015).
- [14] X. Zhong, T. Chervy, S. Wang, J. George, A. Thomas, J. A. Hutchison, E. Devaux, C. Genet, and T. W. Ebbesen, Non-radiative energy transfer mediated by hybrid light-matter states, *Angewandte Chemie International Edition* **55**, 6202 (2016).
- [15] J. Schachenmayer, C. Genes, E. Tignone, and G. Pupillo, Cavity-enhanced transport of excitons, *Phys. Rev. Lett.* **114**, 196403 (2015).
- [16] F. Herrera and F. C. Spano, Cavity-controlled chemistry in molecular ensembles, *Phys. Rev. Lett.* **116**, 238301 (2016).
- [17] R. Sáez-Blázquez, J. Feist, A. Fernández-Domínguez, and F. García-Vidal, Organic polaritons enable local vibrations to drive long-range energy transfer, *Physical Review B* **97**, 241407 (2018).
- [18] C. Schäfer, M. Ruggenthaler, H. Appel, and A. Rubio, Modification of excitation and charge transfer in cavity quantum-electrodynamical chemistry, *Proceedings of the National Academy of Sciences* **116**, 4883 (2019).
- [19] M. Du, L. A. Martínez-Martínez, R. F. Ribeiro, Z. Hu, V. M. Menon, and J. Yuen-Zhou, Theory for polariton-assisted remote energy transfer, *Chemical science* **9**, 6659 (2018).
- [20] J. A. Campos-Gonzalez-Angulo, R. F. Ribeiro, and J. Yuen-Zhou, Resonant catalysis of thermally activated chemical reactions with vibrational polaritons, *Nature Communications* **10**, 1 (2019).
- [21] T. E. Li, J. E. Subotnik, and A. Nitzan, Cavity molecular dynamics simulations of liquid water under vibrational ultrastrong coupling, *Proceedings of the National Academy of Sciences* **117**, 18324 (2020).
- [22] D. Wang, H. Kelkar, D. Martin-Cano, T. Utikal, S. Götzinger, and V. Sandoghdar, Coherent coupling of a single molecule to a scanning fabry-perot microcavity, *Phys. Rev. X* **7**, 021014 (2017).
- [23] O. S. Ojambati, R. Chikkaraddy, W. D. Deacon, M. Horton, D. Kos, V. A. Turek, U. F. Keyser, and J. J. Baumberg, Quantum electrodynamics at room temperature coupling a single vibrating molecule with a plasmonic nanocavity, *Nature Communications* **10**, 10.1038/s41467-019-08611-5 (2019).
- [24] J. Flick, M. Ruggenthaler, H. Appel, and A. Rubio, Atoms and molecules in cavities, from weak to strong coupling in quantum-

- electrodynamics (qed) chemistry, *Proceedings of the National Academy of Sciences* **114**, 3026 (2017), <http://www.pnas.org/content/114/12/3026.full.pdf>.
- [25] X. Li, A. Mandal, and P. Huo, Cavity frequency-dependent theory for vibrational polariton chemistry, *Nature communications* **12**, 1 (2021).
- [26] T. S. Haugland, E. Ronca, E. F. Kjønsstad, A. Rubio, and H. Koch, Coupled cluster theory for molecular polaritons: Changing ground and excited states, *Physical Review X* **10**, 041043 (2020).
- [27] T. S. Haugland, C. Schäfer, E. Ronca, A. Rubio, and H. Koch, Intermolecular interactions in optical cavities: An ab initio qed study, *The Journal of Chemical Physics* **154**, 094113 (2021).
- [28] D. G. Lidzey, D. Bradley, M. Skolnick, T. Virgili, S. Walker, and D. Whittaker, Strong exciton–photon coupling in an organic semiconductor microcavity, *Nature* **395**, 53 (1998).
- [29] E. Peter, P. Senellart, D. Martrou, A. Lemaitre, J. Hours, J. Gérard, and J. Bloch, Exciton-photon strong-coupling regime for a single quantum dot embedded in a microcavity, *Physical review letters* **95**, 067401 (2005).
- [30] X. Liu, T. Galfsky, Z. Sun, F. Xia, E.-c. Lin, Y.-H. Lee, S. Kéna-Cohen, and V. M. Menon, Strong light–matter coupling in two-dimensional atomic crystals, *Nature Photonics* **9**, 30 (2015).
- [31] A. Thomas, E. Devaux, K. Nagarajan, T. Chervy, M. Seidel, D. Hagenmüller, S. Schütz, J. Schachenmayer, C. Genet, G. Pupillo, and T. W. Ebbesen, Exploring superconductivity under strong coupling with the vacuum electromagnetic field, arXiv preprint arXiv:1911.01459 (2019).
- [32] M. A. Sentef, M. Ruggenthaler, and A. Rubio, Cavity quantum-electrodynamical polaritonically enhanced electron-phonon coupling and its influence on superconductivity, *Science advances* **4**, eaau6969 (2018).
- [33] A. Thomas, A. Jayachandran, L. Lethuillier-Karl, R. M. Vergauwe, K. Nagarajan, E. Devaux, C. Genet, J. Moran, and T. W. Ebbesen, Ground state chemistry under vibrational strong coupling: dependence of thermodynamic parameters on the rabi splitting energy, *Nanophotonics* **9**, 249 (2020).
- [34] A. Thomas, L. Lethuillier-Karl, K. Nagarajan, R. M. A. Vergauwe, J. George, T. Chervy, A. Shalabney, E. Devaux, C. Genet, J. Moran, and T. W. Ebbesen, Tilting a ground-state reactivity landscape by vibrational strong coupling, *Science* **363**, 615 (2019).
- [35] H. Hiura, A. Shalabney, and J. George, Cavity catalysis? accelerating reactions under vibrational strong coupling?, chemRxiv (to be published). <https://doi.org/10.26434/chemrxiv.7234721>, v4 (2018).
- [36] J. Lather, P. Bhatt, A. Thomas, T. W. Ebbesen, and J. George, Cavity catalysis by cooperative vibrational strong coupling of reactant and solvent molecules, *Angewandte Chemie International Edition* **58**, 10635 (2019).
- [37] J. Galego, C. Climent, F. J. Garcia-Vidal, and J. Feist, Cavity casimir-polder forces and their effects in ground-state chemical reactivity, *Physical Review X* **9**, 021057 (2019).
- [38] J. A. Campos-Gonzalez-Angulo and J. Yuen-Zhou, Polaritonic normal modes in transition state theory, *The Journal of chemical physics* **152**, 161101 (2020).
- [39] T. E. Li, A. Nitzan, and J. E. Subotnik, On the origin of ground-state vacuum-field catalysis: Equilibrium consideration, *The Journal of Chemical Physics* **152**, 234107 (2020), <https://doi.org/10.1063/5.0006472>.
- [40] X. Li, A. Mandal, and P. Huo, Cavity frequency-dependent theory for vibrational polariton chemistry, *Nature Communications* **12**, 10.1038/s41467-021-21610-9 (2021).
- [41] C. Climent and J. Feist, On the sn2 reactions modified in vibrational strong coupling experiments: reaction mechanisms and vibrational mode assignments, *Physical Chemistry Chemical Physics* **22**, 23545 (2020).
- [42] A. Thomas, L. Lethuillier-Karl, J. Moran, and T. Ebbesen, Comment on on the sn2 reactions modified in vibrational strong coupling experiments: Reaction mechanisms and vibrational mode assignments, ChemRxiv (2020).
- [43] M. Ruggenthaler, J. Flick, C. Pellegrini, H. Appel, I. V. Tokatly, and A. Rubio, Quantum-electrodynamical density-functional theory: Bridging quantum optics and electronic-structure theory, *Phys. Rev. A* **90**, 012508 (2014).
- [44] I. V. Tokatly, Time-dependent density functional theory for many-electron systems interacting with cavity photons, *Phys. Rev. Lett.* **110**, 233001 (2013).
- [45] C. Pellegrini, J. Flick, I. V. Tokatly, H. Appel, and A. Rubio, Optimized effective potential for quantum electrodynamic time-dependent density functional theory, *Phys. Rev. Lett.* **115**, 093001 (2015).
- [46] J. Flick, C. Schäfer, M. Ruggenthaler, H. Appel, and A. Rubio, Ab initio optimized effective potentials for real molecules in optical cavities: Photon contributions to the molecular ground state, *ACS Photonics* **5**, 992 (2018), <https://doi.org/10.1021/acsp Photonics.7b01279>.
- [47] R. Jestädt, M. Ruggenthaler, M. J. Oliveira, A. Rubio, and H. Appel, Light-matter interactions within the ehrenfest–maxwell–pauli–kohn–sham framework: fundamentals, implementation, and nano-optical applications, *Advances in Physics* **68**, 225 (2019).
- [48] J. Flick and P. Narang, Cavity-correlated electron-nuclear dynamics from first principles, *Physical review letters* **121**, 113002 (2018).
- [49] N. Tancogne-Dejean, M. J. Oliveira, X. Andrade, H. Appel, C. H. Borca, G. Le Breton, F. Buchholz, A. Castro, S. Corni, A. A. Correa, *et al.*, Octopus, a computational framework for exploring light-driven phenomena and quantum dynamics in extended and finite systems, *The Journal of chemical physics* **152**, 124119 (2020).
- [50] V. R. Chintareddy, K. Wadhwa, and J. G. Verkade, Tetrabutylammonium fluoride (tbaF)-catalyzed addition of substituted trialkylsilylalkynes to aldehydes, ketones, and trifluoromethyl ketones, *The Journal of organic chemistry* **76**, 4482 (2011).
- [51] T. A. Hamlin, M. Swart, and F. M. Bickelhaupt, Nucleophilic substitution (sn2): dependence on nucleophile, leaving group, central atom, substituents, and solvent, *ChemPhysChem* **19**, 1315 (2018).
- [52] R. Loudon, *The quantum theory of light* (Oxford Science Publications, 1988).
- [53] C. Schäfer, M. Ruggenthaler, V. Rokaj, and A. Rubio, Relevance of the quadratic diamagnetic and self-polarization terms in cavity quantum electrodynamics, *ACS photonics* **7**, 975 (2020).
- [54] C. Schäfer, M. Ruggenthaler, and A. Rubio, Ab initio nonrelativistic quantum electrodynamics: Bridging quantum chemistry and quantum optics from weak to strong coupling, *Physical Review A* **98**, 043801 (2018).

- [55] Y. Pang, A. Thomas, K. Nagarajan, R. M. Vergauwe, K. Joseph, B. Patraha, K. Wang, C. Genet, and T. W. Ebbesen, On the role of symmetry in vibrational strong coupling: the case of charge-transfer complexation, *Angewandte Chemie* **132**, 10522 (2020).
- [56] D. Siedler, C. Schäfer, M. Ruggenthaler, and A. Rubio, Polaritonic chemistry: Collective strong coupling implies strong local modification of chemical properties, *The Journal of Physical Chemistry Letters* **12**, 508 (2020).
- [57] S. Schütz, J. Schachenmayer, D. Hagenmüller, G. K. Brennen, T. Volz, V. Sandoghdar, T. W. Ebbesen, C. Genes, and G. Pupillo, Ensemble-induced strong light-matter coupling of a single quantum emitter, *Physical review letters* **124**, 113602 (2020).
- [58] F. Neese, Software update: the orca program system, version 4.0, *Wiley Interdisciplinary Reviews: Computational Molecular Science* **8**, e1327 (2018).
- [59] J. P. Perdew, K. Burke, and M. Ernzerhof, Generalized gradient approximation made simple, *Physical review letters* **77**, 3865 (1996).
- [60] J. Perdew, K. Burke, and M. Ernzerhof, Perdew, burke, and ernzerhof reply, *Physical Review Letters* **80**, 891 (1998).